Supporting Information

Green Fabrication of High Strength, Transparent Cellulose-based Film with Durable Fluorescence and UV-blocking Performance

Fang Peng, Hongchen Liu*, Dongdong Xiao, Lei Guo, Fengxia Yue, Hendryk Würfel, Thomas Heinze, Haisong Qi*

F. Peng, L. Guo, F. Yue, H. Qi
State Key Laboratory of Pulp and Paper Engineering, South China University of Technology, Guangzhou 510641, China.
E-mail: qihs@scut.edu.cn (Haisong Qi)

H. Liu
State Key Laboratory of Pulp and Paper Engineering, South China University of Technology, Guangzhou 510641, China.
Henan Provincial Key Laboratory of Functional Textile Materials, Zhongyuan University of Technology, Zhengzhou 450007, China
E-mail: liuhongchen.beyond@163.com (Hongchen Liu)

D. Xiao
Department of Urology and Andrology, Ren Ji Hospital, School of Medicine, Shanghai Jiaotong University, Shanghai 200001, China

H. Würfel, T. Heinze
Center of Excellence for Polysaccharide Research, Institute of Organic Chemistry and Macromolecular Chemistry, Friedrich-Schiller-University of Jena, Humboldtstr. 10, D-07743 Jena, Germany

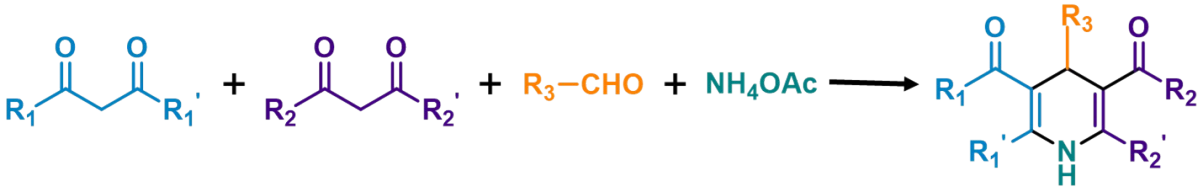

Scheme S1. Hantzsch reaction. Bimolecular β -ketoate esters are condensed with one molecule of aldehyde and one molecule of ammonia, respectively, to obtain corresponding intermediates. The two intermediates are cyclized to form dihydropyridine derivatives through intramolecular addition - elimination reaction.[1, 2]

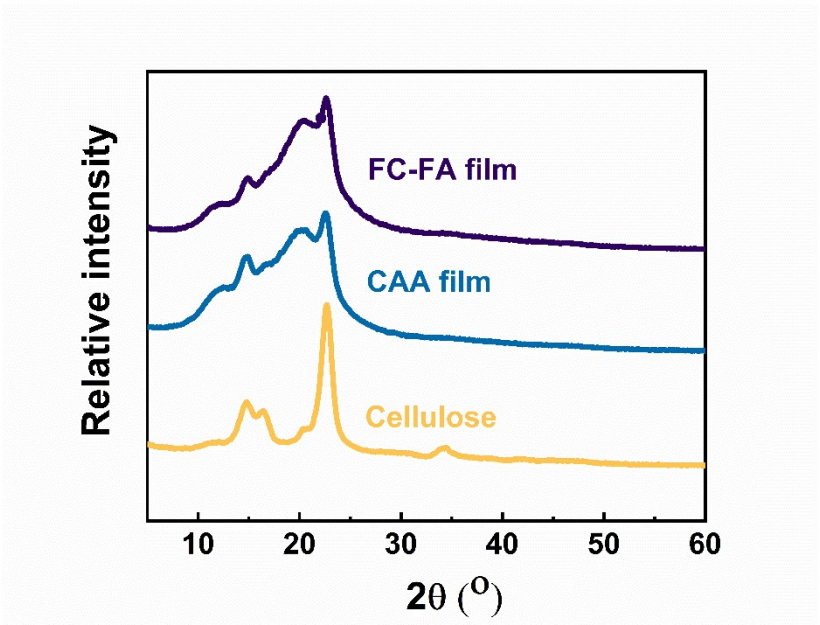

Figure S1. XRD patterns of cellulose, CAA film and FC-FA film.

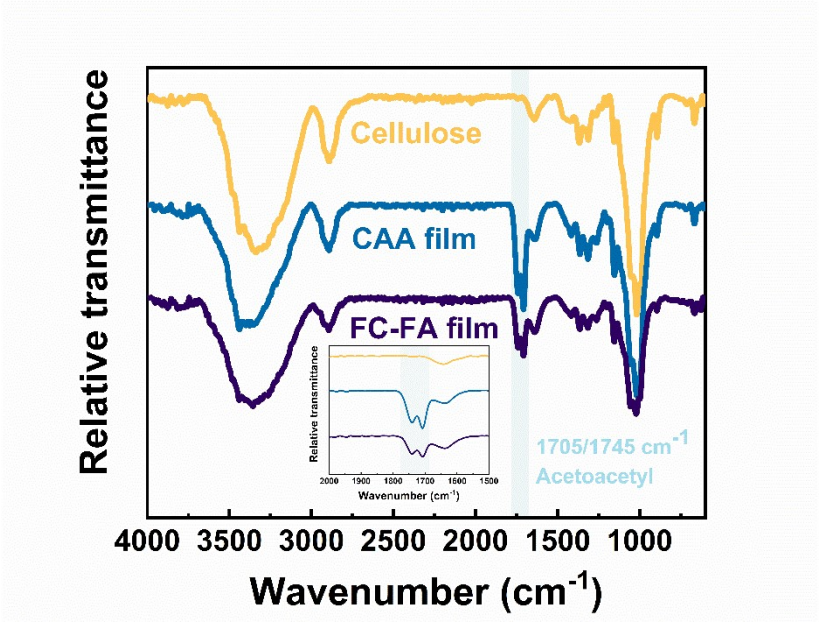

Figure S2. FT-IR spectra of cellulose, CAA film and FC-FA film.

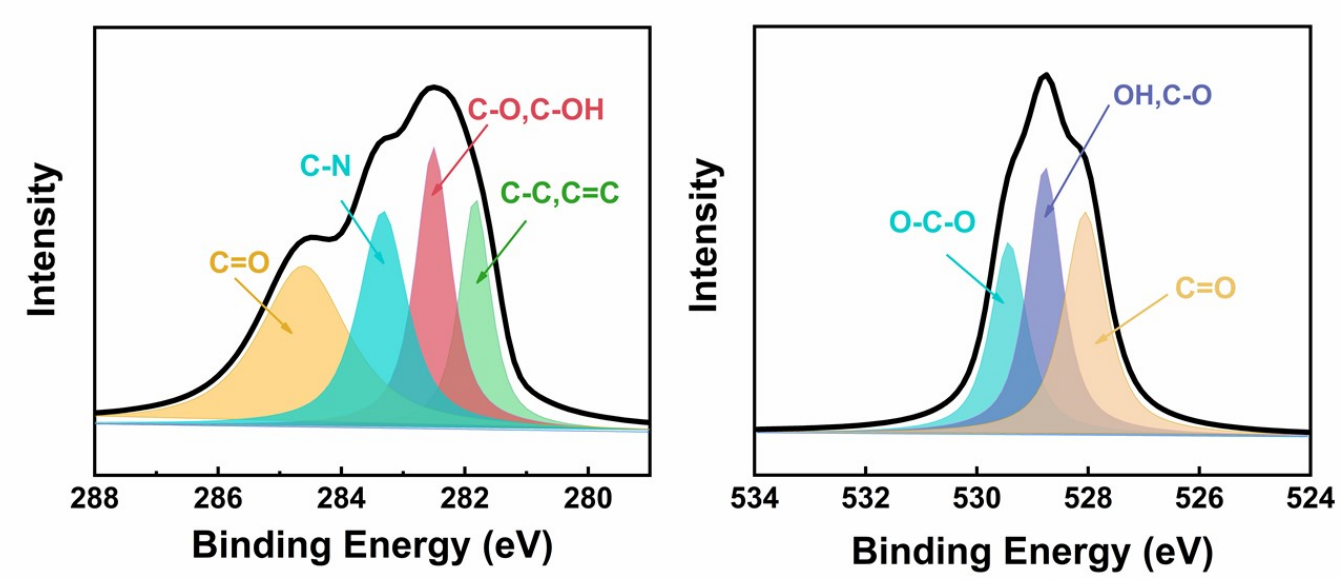

Figure S3. (A) High-resolution XPS C 1s spectra (B) O 1s spectra of FC-FA film.

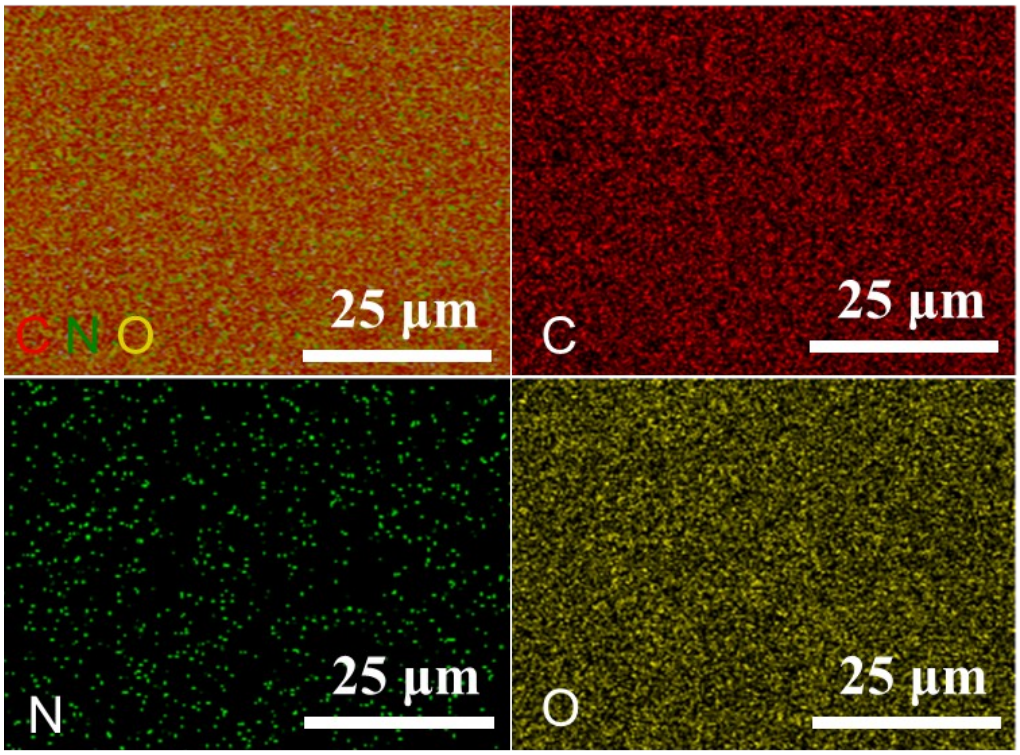

Figure S4. EDS elemental mapping images C, N, O of FC-FA film.

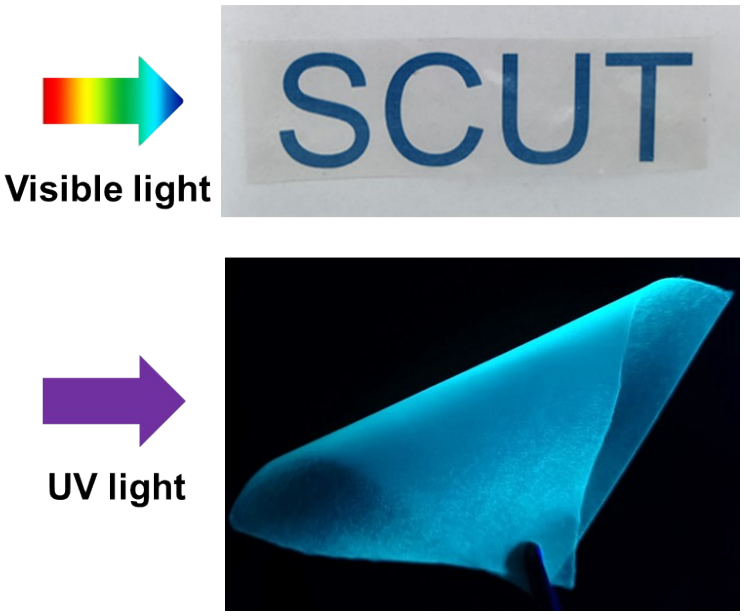

Figure S5. Digital image of FC-FA films under visible light and UV irradiation (365 nm).

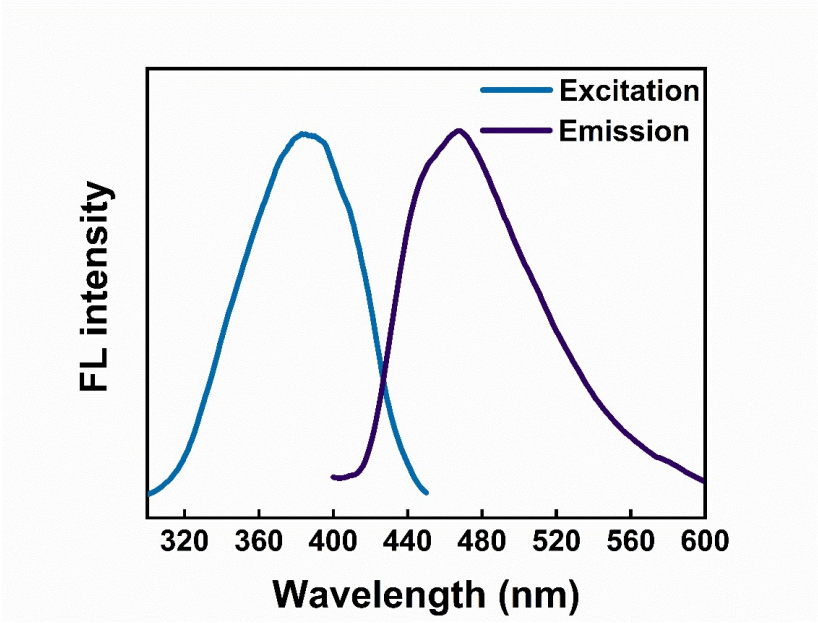

Figure S6. Fluorescence spectra of the FC-FA film.

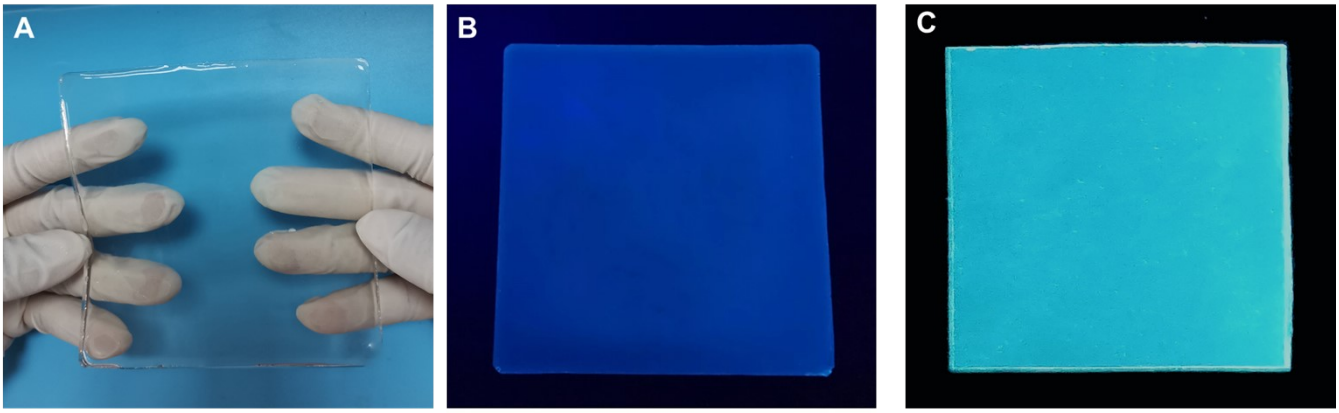

Figure S7. Digital image of FC-FA hydrogel film under (A) visible light and (B) UV light (365nm). (C) Digital image of FC-FA film under UV light (365nm).

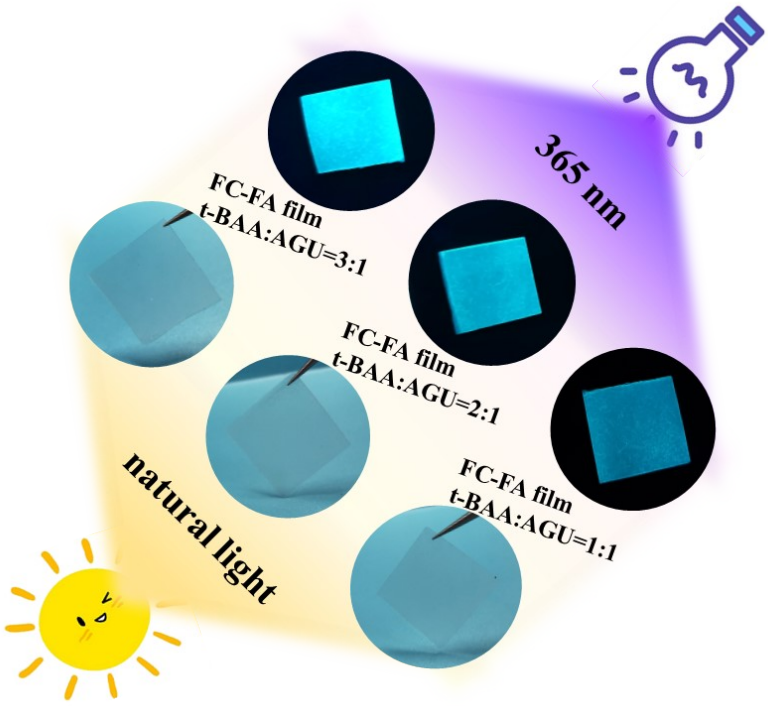

Figure S8. Digital image of FC-FA films under visible light and UV irradiation (365 nm) with increasing acetoacetyl moieties.

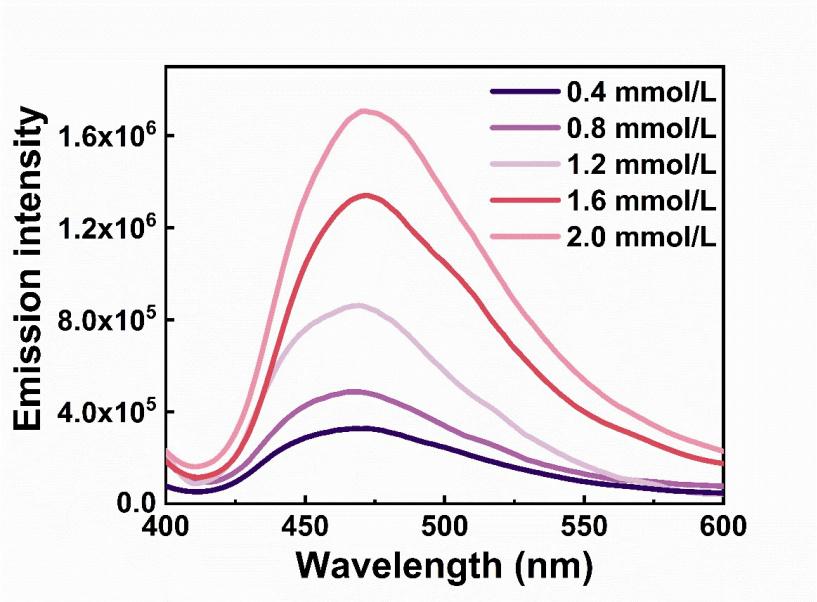

Figure S9. Emission intensity of FC-FA film with increasing aldehyde concentration.

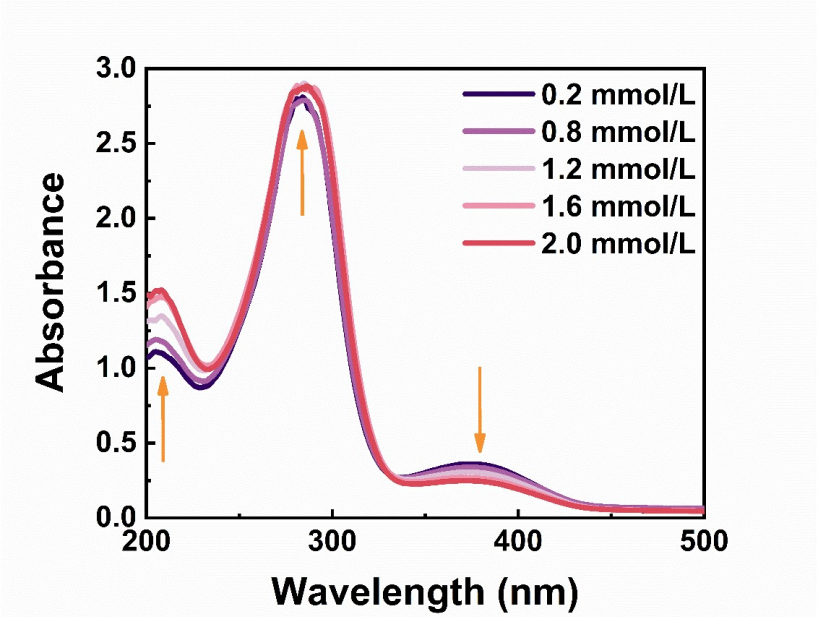

Figure S10. UV-vis absorption spectra emission spectra of FC-FA film with increasing aldehyde concentration.

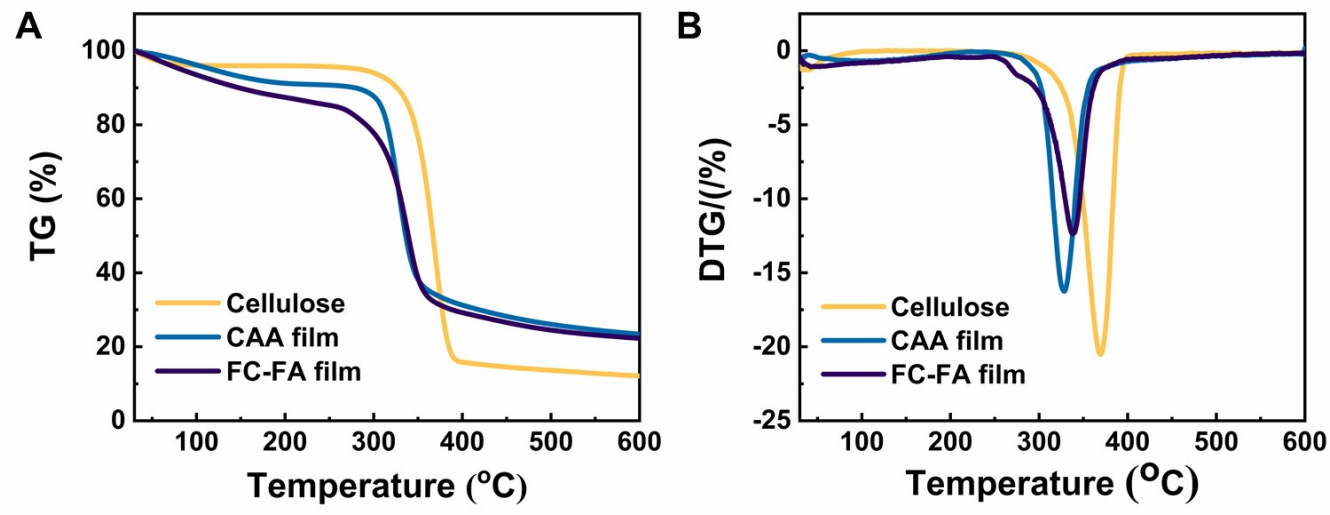

Figure S11. (A) TG and (B) DTG curves of the cellulose, CAA film and FC-FA film.

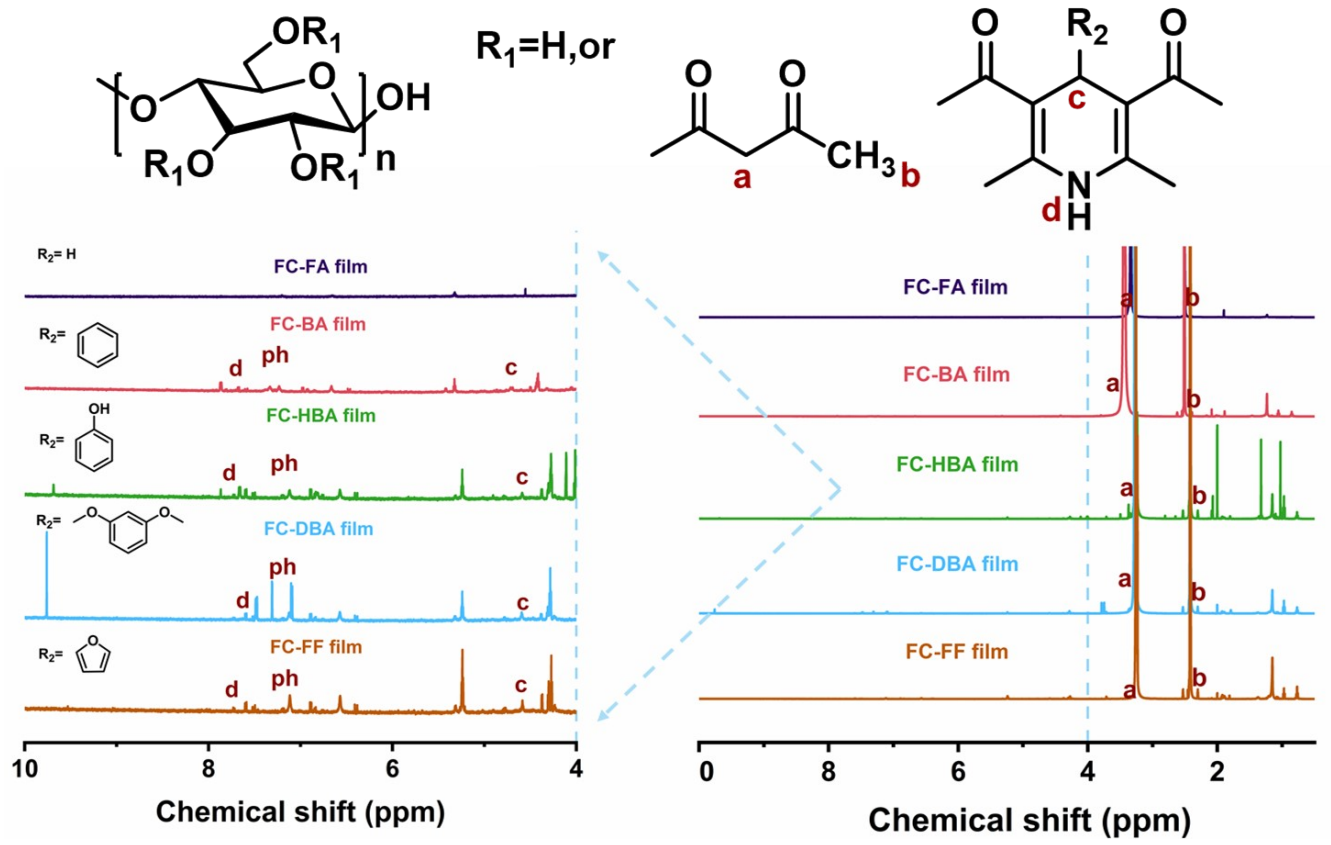

Figure S12. ^{1}H NMR spectra (DMSO-d_6, 600M) of fluorescent cellulose films.

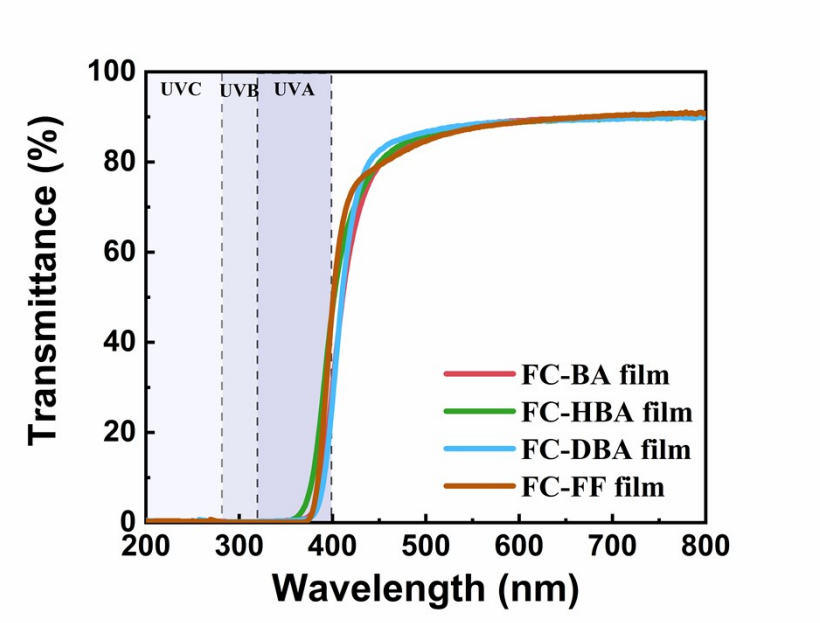

Figure S13. UV-vis transmittance emission of fluorescent cellulose film after UV irradiation (340 nm, 0.89 W m^{-2}) at 60℃ for 24 h.

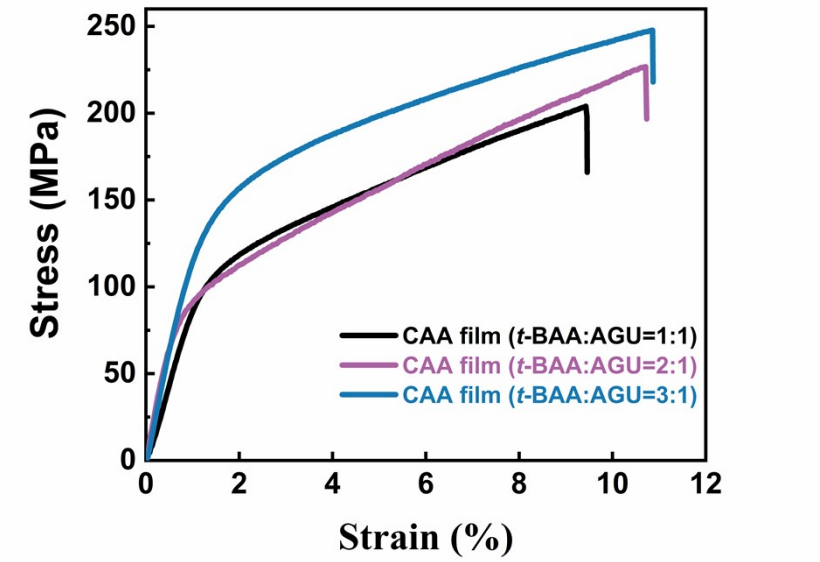

Figure S14. Stress−strain curves of CAA films with increasing acetoacetyl moieties.

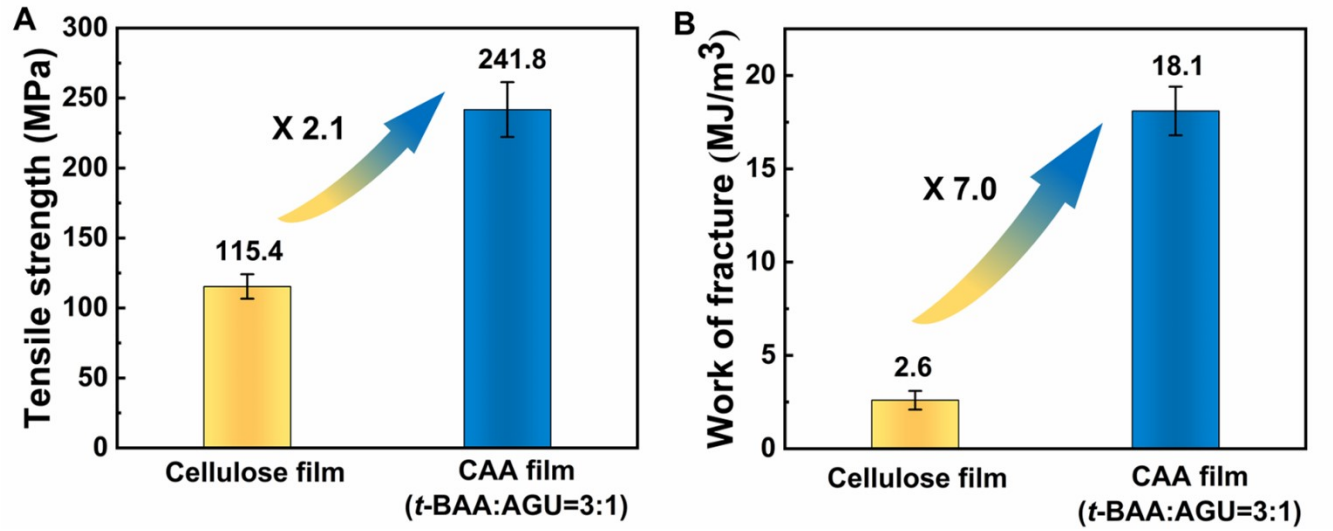

Figure S15. (A) The strength and (B) toughness of the cellulose film and CAA film (*t*-BAA: AGU =3:1).

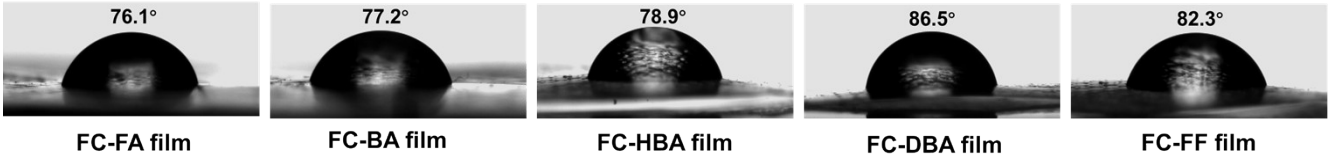

Figure S16. Photographs of water droplets on the fluorescent cellulose films.

Figure S17. Fluorescent anti-counterfeiting of films under UV irradiation (365 nm)

Notes and references

1. G. Q. Liu, R. H. Pan, Y. Wei and L. Tao, *Macromol Rapid Comm*, 2021, **42**, 2000459.

2. H. G. O. Alvim, E. N. da Silva and B. A. D. Neto, *Rsc Adv*, 2014, **4**, 54282-54299.